Large Area Picosecond Photodetector (LAPPD) Performance Test Results

Michael J. Minot, Mark A. Popecki, and Matthew J. Wetstein,

***Abstract* - We report and review performance test results achieved for recently produced fully functional sealed Large Area Picosecond Photodetectors (LAPPD™) in tests performed at Incom Inc., as well as independent test results reported by our early adopters. Results for LAPPD#37 include electron gains ≥ 9 x10^6 @ 900V/MCP and 1X10^7 @925V/MCP and 30V between the photocathode and top of the top MCP, low dark count rates (64 Cts/s cm^2), and a mean photocathode QE (#37) of 19.3%. Single photoelectron temporal and spatial time resolutions, typically achieved for first generation LAPPD are also reported. We will conclude with examples of how sensors offering picosecond timing, in diverse applications such as particle and astro-particle physics, Cherenkov imaging, medical imaging, fast imaging, homeland security systems and neutron imaging can bring transformative change to detector technology and applications in future experiments.**

I. INTRODUCTION

A. *Relevant Background*

The LAPPD™ is a microchannel plate (MCP) based large area picosecond photodetector, capable of imaging with single-photon sensitivity at high spatial and temporal resolutions in a hermetic package. The LAPPD™ has an active area of 350 square centimeters when X-spacers and edge frames are accounted for, in an all-glass hermetic package with top and bottom plates and sidewalls made of borosilicate float glass. Signals are generated by a bi-alkali Na_2KSb photocathode and amplified with a stacked chevron pair of ALD-GCA-MCPs produced by applying resistive and emissive atomic layer deposition coatings to bare glass capillary array (GCA) substrates. Signals are collected on RF strip-line anodes applied to the bottom plates which exit the detector via pin-free hermetic seals under the side walls.

The US Department of Energy funded Incom Inc. in 2014 to demonstrate a pathway for commercialization of LAPPD™ as well as the large area ALD-GCA-MCPs that enable these photodetectors[1],[2],[3]. Custom equipment and facilities were designed and implemented allowing equipment and process commissioning trials to commence in November 2015. Early commissioning trials demonstrated the ability to successfully seal LAPPDs[4], to apply uniform high QE photocathodes over the full area of the window, to achieve high gain from the chevron pair of ALD-GCA-MCPs, and to produce well-formed single photoelectron (PE) pulse height distributions.

Manuscript received December 19, 2018. This work supported by U. S. Department of Energy, Office of Science, Office of Basic Energy Sciences, Offices of High Energy Physics and Nuclear Physics under DOE contracts: DE-SC0009717; DE-SC0011262, and DE-SC0015267.

Michael J Minot is Director Research and Development with Incom Inc., Charlton, MA. USA Telephone 508-909-2369 E-mail mjm@incomusa.com

Mark A. Popecki is Senior Research Scientist with Incom Inc., Charlton, MA. USA Telephone; 508-909-2306 E-mail: map@incomusa.com

Matthew J. Wetstein is Assistant Professor, with Iowa State University, Ames, IA 50011Telephone: 515-294-8269 E-mail: wetstein@iastate.edu

These early trials culminated in the fall of 2017 with the fabrication of tiles that achieved all of these parameters at usable levels, in the same fully functional LAPPDs. While process optimization continues, these successes are now enabling the LAPPD to be fabricated on a regular pilot production basis and to be made available to early adopter users, for evaluation and test, as described here and in earlier publications[5].

B. *LAPPD Performance Test Methods*

LAPPD performance tests were performed in a dark box with a UV light source and signal acquisition hardware. LAPPD are provided with an Ultem housing that provides high voltage connections, and a backplane that connects anode strips to SMA connectors with near-50 ohm impedance, as shown in Fig. 1. Detail measurement and test reports, available on-line, show recommended high voltage connections that separate current paths of the entry and exit MCPs, so anomalies in either may be detected and allowing photocathode voltage to be controlled independently of the MCPs[6].

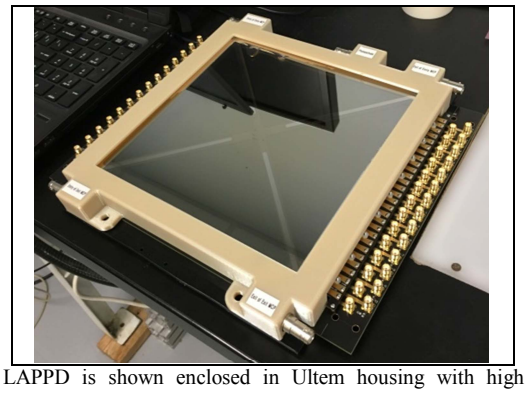

Fig. 1- LAPPD is shown enclosed in Ultem housing with high voltage connectors, mounted on a backplane for signal access.

Quantum efficiency of the photocathode was measured across the LAPPD window by scanning a 365 nm UV LED in an XY pattern of 3 mm steps. The illumination on the window had a circular pattern with a ~2.5 mm diameter. The intensity of the input light was measured with a Thorlabs SM1PD2A photodiode, and a Keithley 2410 picoammeter. The photocurrent was collected and measured by connecting both sides of the entry MCP to a Keithley 6485 picoammeter, with a 42 volt bias voltage between the MCP and the photocathode. The quantum efficiency is calculated from the ratio of these two quantities, less the dark current in each. The UV LED source was stepped across the LAPPD window and at each step, the input light intensity and resulting photocurrent was measured.

Gain was measured as a function of MCP voltage, using two PSI DRS4 evaluation boards, obtaining a waveform for

978-1-5386-8495-5/18/$31.00 ©2018 IEEE

each MCP pulse, and then measuring the area under each pulse[7]. MCP pulses were produced by directing a 405 nm PiLas 20 picosecond UV pulsed laser to a selected point on the LAPPD window. The laser was triggered externally at 11.6 kHz. A neutral density filter (NE513B from Thorlabs) and a polarization filter were used on the laser to reduce the intensity to the single photon level. At this level, the LAPPD responded to 3 out of every 20 laser pulses.

The transit time variation between the initiation of a photoelectron and the arrival of the MCP pulse at the end of a strip is of interest for timing applications. This variation represents the timing uncertainty of the LAPPD. The time variation was measured by using a fast photodiode to directly monitor the 405 nm laser pulse. The time difference between the monitor pulse and the corresponding pulse from a single strip was measured using the DRS4 waveform samplers. The variation in this time is the transit time variation of the LAPPD. Variations may come from phenomena such as the depth to which the photoelectron advances into the microchannel before striking the walls of the channel. Additional variations arise from electronic noise superimposed on the strip measurement, and on the photodiode waveform. There is also a ~±25 pS jitter in the width of the DRS4 time steps, which is not corrected here. For these reasons the quality of the measurement is dependent on the test setup and hardware available, and the result here are not the best achievable with the LAPPD.

II. RESULTS

LAPPD #37 performance is summarized in Table 1.

Table 1 – Summary of LAPPD #37 Performance

Parameter	Performance
MCP resistance, Entry/Exit; MΩ	11.5 / 5.5 / at 875 V
PC QE% @365nm: Max, Mean	21.7 / 19.3
PC QE% Spatial Variability, σ	3
LAPPD Gain @ 900V/MCP, 30V@ PC @ 925V/MCP, 30V@ PC	 9 X10^6 1 X10^7
Tile Dark Count Rate @850 V/MCP and 30 V on PC @875 V/MCP and 30 V on PC	 0.064 kHz/cm^2 18 kHz/cm^2
Single P/E TTS (provisional)	97 psec

The QE map for LAPPD #37 is shown in Fig. 2.

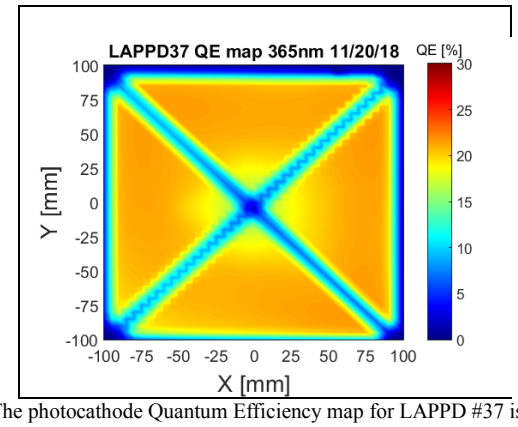

Fig. 2. The photocathode Quantum Efficiency map for LAPPD #37 is shown at 365 nm. The average QE is 19.3%, +- 3%. The maximum QE is 21.7%.

The maximum quantum efficiency at 365 nm is 21.7%. The average QE at 365 nm is 19.3%, with a sigma of 3% absolute. The X-spacers are visible in the map.

Single PE peaked pulse height distributions, plotted as Gain for different MCP voltages as measured with the DRS4s, is shown in Fig. 3 (left). Gain vs. MCP Voltage Fig. 3 (right) is the average of the pulse height distributions shown in the left panel. The photocathode voltage was 30 volts. The gain derived from the DRS4 samples at 900 V/MCP was 9 X 10^6 and was as high as 1 X 10^7 at 925 Volts / MCP.

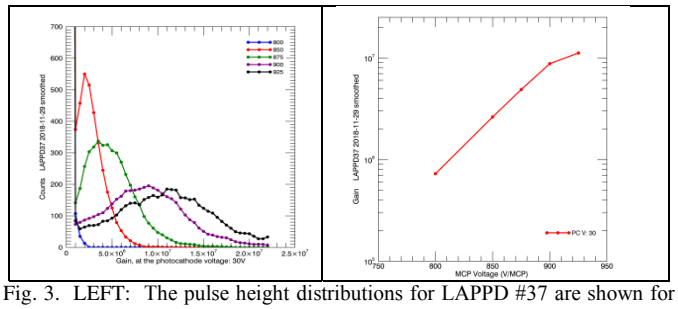

Fig. 3. LEFT: The pulse height distributions for LAPPD #37 are shown for 30 V on the photocathode. The distributions are well-separated from threshold at 875 V/MCP or more. RIGHT: Gain vs. MCP voltage, the gain is as high as 1X10^7 at 925 V/MCP.

C. *Dark rates vs. MCP and photocathode voltage*

Dark rates are shown in Fig. 4 as a function of MCP voltage and photocathode voltage.

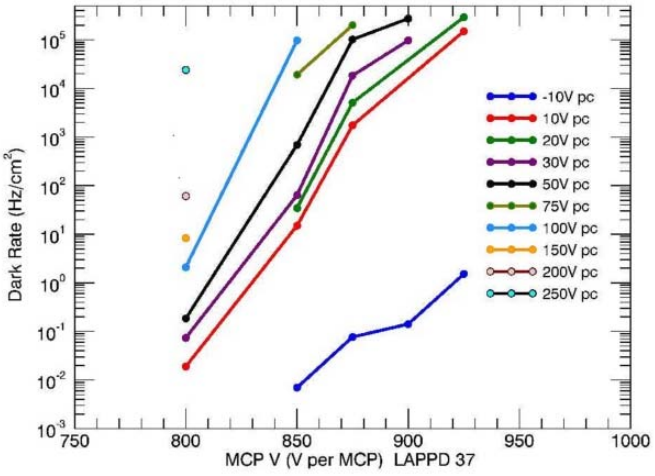

Fig. 4. Dark rates for LAPPD #37 are shown as a function of MCP and photocathode voltage

Higher photocathode and MCP voltages tend to increase the gain, but they also increase the dark rates. These rates were acquired from a single 13.5 cm^2 strip.

D. *Position of Charge, and Spatial Resolution*

MCP charge deposition position and spatial resolution may be measured with the LAPPD strip line anode in two ways. Along a strip, the position of the charge pulse may be inferred by measuring the relative time of arrival of pulses at each end of the strip, as the charge deposited by the MCP makes its way to ground at both ends. Position may be measured across strips by measuring the centroid of three adjacent strip signals,

resulting in the position to a better resolution than the strip pitch itself. The along strip resolution for LAPPD #31 was 2.4 mm RMS and 0.76mm RMS for across strip resolution. The results of these measurements are representative of the current first generation LAPPD design, using 20-micron MCPs, with the currently used gap spacing from the photocathode to the top of the top MCP, between MCPs and the gap between the bottom of the bottom MCP and the anode strips. For this reason, these measurements were not repeated for LAPPD #37.

E. Transit Time Variation

Transit time variation measurements for LAPPD #37 were made with an MCP voltage of 925 V/MCP, and 30 V on the photocathode. The 405 nm laser that is used for the LAPPD tests has a 20 psec firing window. The intensity is reduced by neutral density filters to produce single photoelectrons. Therefore, the laser photon that produces the single electron may arrive at any time within the 20 psec window. The transit time distribution is shown in Figure 5.

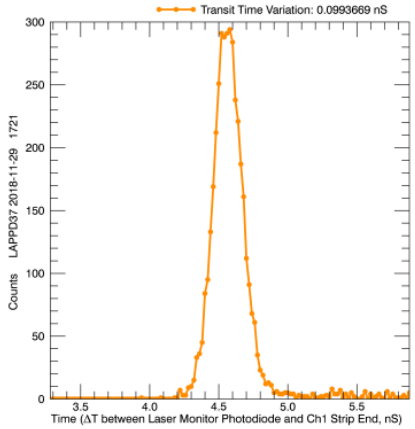

Figure 5 - A 97 psec transit time variation for LAPPD #37 is observed. This is the time difference between the observed laser firing and the arrival of the MCP pulse at the end of an anode strip

The standard deviation of the distribution is 99 psec. If the variation of the laser photon has a standard deviation of 20 psec, then the LAPPD transit time variation may be extracted as a sum of squared variations as 97 psec: $\sigma_{Meas}^2 = \sigma_{LAPPD}^2 + \sigma_{LaserWidth}^2$.

In addition to the tests completed at Incom Inc., earlier tests were done on LAPPD #25 at the Iowa State University, on behalf of the ANNIE collaboration[8]. ANNIE testing was done in a dark box, with motorized optics allowing for position scans, similar to Incom's. ANNIE testing had the availability of a PiLas laser with up to 30 psec resolution, a 10 GHz, 20 Gs/sec scope, and PSEC4 electronics, allowing them to do preliminary rise time and transit time spread testing. Those measurements gave a transit time spread (TTS) of 64 psec.

III. Discussion & Conclusions

Routine pilot production of all-glass LAPPDs is now underway at Incom Inc. Table 2 provides a summary of recent tiles supplied to early adopters. Multiple tiles tested at Incom Inc., as well as at early adopter facilities exhibit "target" performances with Gain > 7X10^6 or higher, mean PC QE > 19%, with time and spatial resolution of < 70 Psec, and < 3 mm respectively. Manufacturing scale-up challenges remain to achieve all of these performances in the same tile. Prototypes still exhibit artifact features that will be resolved in coming months as production volume and experience increases. Technical challenges currently being addressed include achieving PC QE targets ≥ 20% consistently from run to run, eliminating high voltage limitations on achieving the full gain available with the ALD-GCA-MCPs being used, understanding and resolving how high PC and MCP voltages impact dark count rates, and design optimizations for enhanced spatial and timing resolution, including implementation of smaller pore ALD-GCA-MCPs. Despite these limitations, the early LAPPD currently available are providing early adopters a means to explore the potential of pico-second timing for their applications.

Table 2 – Performance Test Result Summary

Parameter	LAPPD 31	LAPPD 35	LAPPD 37
Mfg. Date	5/25/2018	9/19/2018	11/13/2018
MCP resistance (Entry/Exit; M•)	9.7 / 10.5 @900 V	9.2 / 7.6 @925 V	11.5 / 5.5 @875 V
QE % @365 nm Max/Mean/σ	14 /9.8/1.1	2.6/**1.3**/ 0.5	21.7/**19.3** 3
Gain 30 V on PC	8.0 X10^6 @ 925/925 V (entry/exit)	8.4 X10^6 @925 V/MCP	9X10^6 @900 V/MCP
Dark rate; @ 8E5 gain, +30 PC V	14 Cts/s-cm^2 @ 900 V/MCP	38 Cts/s-cm^2 @900 V/MCP 0.799 kHz/cm^2 @925 V/MCP,	64 Cts/s-cm^2 @850 V/MCP 18 kHz/cm^2 @875 V/MCP,
After pulses	Very few	Very few	Very few
Along-strip **Spatial Resolution** Cross-strip	2.4 mm RMS 0.76mm RMS	1.8 mm RMS 0.78 mm RMS	Not Measured
SPE psec, **TTS** ~20 PE psec,	99 -	134 102	97 -

Fast timing enables many benefits for high energy and nuclear physics experiments including 1) more efficient background rejection, 2) high vertex resolution in large scale experiments, 3) separation of Cherenkov and scintillation light, 4) directionality information, 5) precise track reconstruction, as well as others. Multiple applications for particle detection in accelerator physics, collider physics, neutrinoless double beta decay and nuclear physics have been identified[9],[10],[11],[12]. The availability of low cost, large area photodetectors that offer picosecond-scale timing is expected to have a transformative effect on the way future experiments will be conducted. In one recent demonstration[13], mirrors and picosecond timing were used to effectively double the photo-detection efficiency while providing a time-resolved image of the Cherenkov light on the opposing wall. Application of particular interest for evaluation of LAPPD include ANNIE (Atmospheric Neutrino Neutron Interaction Experiment), Neutron imaging detectors, TOF trials on the Fermilab beam

line, WATCHMAN, THEIA, REDTOP, EIC and others. It is expected that as end users become more familiar with the benefits of picosecond-level timing, additional applications will be identified.

REFERENCES

1 H.J. Frisch, et al, "A brief technical history of the large-area picosecond photodetector (LAPPD) collaboration", arXiv:1603.01843.

2 J. W. Elam, A. U. Mane, J. A. Libera, J. N. Hryn, O. H. W. Siegmund, Jason McPhate, M. J. Wetstein, A. Elagin, M. J. Minot, A. O'Mahony, R. G. Wagner, W. M. Tong, A. D. Brodie, M. A. McCord, and C. F. Bevis, "Synthesis, characterization, and application of tunable resistance coatings prepared by atomic layer deposition," ECS Transactions, 58 (10) 249-261 (2013).

3 J. W. Elam, A. U. Mane, "Tunable resistance coatings," US Patent Number 8,921,799 B2, Issued December 30, 2014; US Patent Number 9,105,379 B2, issued August 11, 2015.

4 M. J. Minot, et al., "Pilot production & commercialization of LAPPD™," Nucl. Instrum. Methods A, 787:78–84, 2015.

5 M. J. Minot, et al., "Large area picosecond photodetector (LAPPD™) Pilot production and development status," https://doi.org/10.1016/j.nima.2018.11.137

6 http://www.incomusa.com/mcp-and-lappd-documents/

7 https://www.psi.ch/drs/evaluation-board

8 http://annie.fnal.gov/

9 A. R. Back et al., "Accelerator neutrino neutron interaction experiment (ANNIE): Preliminary results and physics phase proposal," arXiv:1707.08222.

10 A. Elagin et al., "Separating double-beta decay events from solar neutrino interactions in a kiloton-scale liquid scintillator detector by fast timing," Nucl. Instr. Meth. Phys. Res. A849 (2017) 102.

11 C. Aberle, A. Elagin, H. J. Frisch, M.J. Wetstein, L. Winslow, "Measuring directionality in double-beta decay and neutrino interactions with kiloton-scale scintillation detectors, JINST 9 P06012 (2014).

12 J. Caravaca et al., "Probing Cherenkov and scintillation light separation for next-generation neutrino detectors," J.Phys.Conf.Ser. 888 (2017) no.1, 012056.

13 E. Oberla and H.J. Frisch, "The design and performance of a prototype water Cherenkov optical time-projection chamber" NIM 814 (2016) https://arxiv.org/abs/1510.00947 .